

January 2003
DAMTP-2003-8
hep-th/0301166

Graphical Representation of Supersymmetry

Shoichi ICHINOSE¹

Department of Applied Mathematics and Theoretical Physics,
University of Cambridge,
Wilberforce Road, Cambridge, CB3 0WA, UK.

Abstract

A graphical representation of supersymmetry is presented. It clearly expresses the chiral flow appearing in SUSY quantities, by representing spinors by directed lines (arrows). The chiral indices are expressed by the directions (up, down, left, right) of the arrows. The $SL(2, \mathbb{C})$ invariants are represented by wedges. Both the Weyl spinor and the Majorana spinor are treated. We are free from the messy symbols of spinor indices. The method is applied to the 5D supersymmetry. Many applications are expected. The result is suitable for coding a computer program and is highly expected to be applicable to various SUSY theories (including Supergravity) in various dimensions.

PACS NO: 02.10.Ox, 02.70.-c, 02.90.+p, 11.30.Pb, 11.30.Rd,

Key Words: Graphical representation, Supersymmetry, Spinor space, Chiral space, Graph index

¹On leave of absence from School of Food and Nutritional Sciences, University of Shizuoka, Yada 52-1, Shizuoka 422-8526, Japan (Address after Feb. 9, 2003).
E-mail address: ichinose@u-shizuoka-ken.ac.jp

1 Introduction

Since supersymmetry was born, more than quarter century has passed. Although super particles are not yet discovered in experiments, everybody now admires its importance as one possible extension beyond the standard model. Some important models, such as 4 dimensional $N = 4$ susy YM, give us a deep insight in the non-perturbative aspects of the quantum field theories. Because of the high symmetry, the dynamics is strongly constrained and it makes possible to analyse the nonperturbative aspects. The BPS state is such a representative.

The beauty of SUSY theory comes from the harmony between bosons and fermions. At the cost of the high symmetry, the SUSY fields generally carry many indices: chiral superfields (ϕ), anti-chiral superfields ($\bar{\phi}$) in addition to usual ones: gauge superfields ($i; j; ::$), Lorentz superfields ($m; n; \dots$). The usual notation is, for example, $\overset{\overset{1}{\wedge}}{m} \dots$. Many superfields are "crowded" within one character \wedge . Whether the meaning of a quantity is clearly read, sometimes crucially depends on the way of description. In the case of quantities with many indices, we are sometimes lost in the "jungle" of superfields. In this circumstance we propose a new representation to express SUSY quantities. It has the following properties.

1. All superinformation is expressed.
2. Superfields are suppressed as much as possible. Instead we use the "geometrical" notation: lines, arrows, ² particularly, contracted superfields (we call them "dummys" superfields) are expressed by vertices (for fermion superfields) or lines.
3. The chiral flow is manifest.
4. The graphical indices specify a spinorial quantity.

Another quantity with many superfields is the Riemann tensor appearing in the general relativity. It was already graphically represented [1] and some applications have appeared [2, 3].

We follow the notation and the convention of the textbook by Wess and Bagger[4]. Many (graphical) relations appearing in the present paper (except Sec.6 and Sec.8) appear in that textbook.

2 Definition

2.1 Basic Ingredients

Let us represent the Weyl fermion ψ_α ($\alpha = 1, 2$) and their 'super-raised' partners as in Fig.1. Raising and lowering the spinor superfields is done by the antisymmetric tensors γ^μ :

$$= \quad ; \quad \gamma^\mu = \gamma^\mu \quad ; \quad \gamma^{12} = \gamma_{21} = 1 \quad ; \quad (1)$$

²In this sense, the use of "forms" instead of the tensorial quantities is the similar line of simplification.

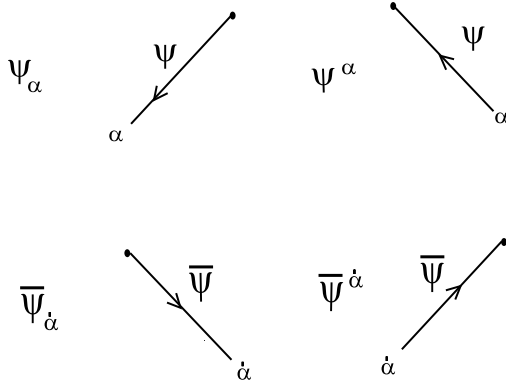


Figure 1: Weyl fermions.

where and are in the inverse relation: $\psi_\alpha = \psi^\alpha$.

Graphical Rule 1 (Fig.1)

1. The arrow is pointed to the left for the chiral field and to the right for the anti-chiral one. (Complex structure)
2. The arrow is pointed to the up for the upper-su₂ x quantity and to the down for lower-su₂ x quantity. (Symplectic structure)
3. All spinor su₂ xes (; ; ;) are labeled at the lowest position of arrow lines.

The choice of 3 is fixed by the condition that, when we express the basic $SL(2, C)$ (Lorentz) invariants (NW -SE convention) = $\psi_\alpha \psi^\alpha$, (SW - NE convention) = $\psi_\alpha \psi^\alpha$ where su₂ xes are contracted by the anti-symmetric tensor³, the arrows continuously flow along the lines (see Fig.4 which will be explained later) without changing the order of the spinor-field graphs.

Graphical Rule 2

Every spinor graph is anticommuting in the horizontal direction.

The derivatives of fermions are expressed as in Fig.2. We give it as a rule.

Graphical Rule 3 (Fig.2)

1. For each derivative, attach the derivative symbol " ∂ " to the corresponding spinor-arrow with a dotted line as in Fig.2. At the end of the line, the Lorentz su₂ x of the derivative is described.
2. The order of the derivative lines described above is irrelevant because the derivative ∂ is commutative.

Following the above rule, the elements of the $SL(2, C)$ matrix are expressed as in Fig.3. In Fig.3, the two arrows are directed 'horizontally outward' for ψ_α , whereas 'horizontally inward' for ψ^α . We consider $(^m)_+$ and $(^m)_-$ are the

³NorthWest-SouthEast (NW -SE), SouthWest-NorthEast (SW -NE).

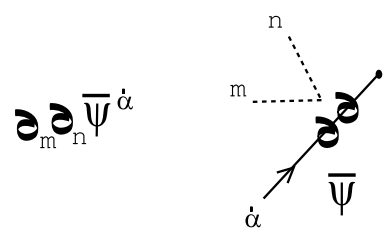
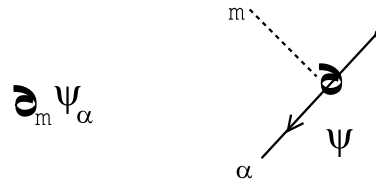


Figure 2: Derivatives of fermions.



Figure 3: Elements of $SL(2, \mathbb{C})$ -matrices. $(^m)_-$ and $(^m)_+$ are the standard form.

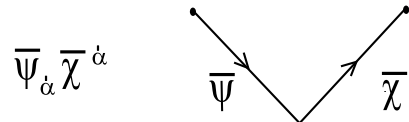
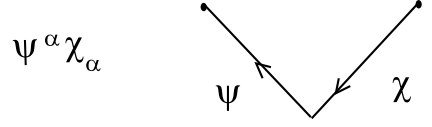


Figure 4: Contraction of spinor su(2) x (es). [above] N (orth)-W (est)-S (outh)-E (ast) contraction for the chiral ψ (ψ^α = ψ_α) : [below] SW - NE contraction for the anti-chiral $\bar{\psi}$ ($\bar{\psi}_\alpha$ = $\bar{\psi}^\alpha$).



Figure 5: Two Lorentz vectors $(\sigma^m)_{\alpha\beta}$ and $(\bar{\sigma}^m)_{\alpha\beta}$. The double wedge structure appears.

standard form which is basically used in this text.

2.2 Spinor su(2) x contraction

Lorentz covariants and invariants are expressed by the contraction of the spinor su(2) x (es). We take the convention of NW -SE contraction for the chiral ψ (ψ^α = ψ_α), and SW - NE contraction for the anti-chiral one $\bar{\psi}$. They are expressed by connecting the corresponding su(2) x-ends as in Fig.4. The wedge structure, in Fig.4, characterizes all spinor contractions in the following. For the chiral-su(2) x (es) contraction, the wedge 'runs' to the left, whereas the anti-chiral ones to the right.

Graphical Rule 4: Spinor Su(2) x Contraction (Fig.4)
The contraction is expressed by connecting the corresponding su(2) x-ends.

Two Lorentz vectors, $(\sigma^m)_{\alpha\beta}$ and $(\bar{\sigma}^m)_{\alpha\beta}$ are expressed as in Fig.5. The double-wedge structure, in Fig.5, characterizes the vector quantities which involve one σ^m or one $\bar{\sigma}^m$.

$$(\sigma^n)_{\alpha\dot{\alpha}} (\bar{\sigma}^m)^{\dot{\alpha}\beta}$$

$$(\bar{\sigma}^n)^{\dot{\alpha}\alpha} (\sigma^m)_{\alpha\dot{\beta}}$$

Figure 6: $(\sigma^n)_-$ $(\bar{\sigma}^m)_-$ and $(\bar{\sigma}^n)_-$ $(\sigma^m)_-$. The "spinor contraction" between and is expressed as a wedge.

$$\xi^\alpha (\sigma^m)_{\alpha\dot{\beta}} \partial_m \bar{\Psi}^{\dot{\beta}}$$

Figure 7: A Lorentz invariant: $(\sigma^m)_- \partial_m -$.

Next we take examples with two 's. $(\sigma^n)_-$ $(\bar{\sigma}^m)_-$ and $(\bar{\sigma}^n)_-$ $(\sigma^m)_-$ are expressed as in Fig.6. The "spinor contraction" between and is also expressed as a wedge.

Graphical **R**ule 5: **S**pace-**T**ime **S**pace **S**u xes **C**ontraction
The contraction of space-time su xes is expressed by a dotted line.

An example $(\sigma^m)_- \partial_m -$ is expressed as in Fig.7. Note that all dummy su xes do not appear in the final invariant quantities.

The contraction is expressed by the directed wedges and the dotted curved lines.

This makes the expression very transparent.

As the partially contracted examples, we take $(\sigma^n)_-$ and $(\bar{\sigma}^m)_-$. See Fig.8. The spinor su xes σ^n and the space-time su xes remain and wait for further contraction.

2.3 Graphical Formula

An important advantage of the graphical representation is the usage of graphical formula (relations). It helps so much in practical calculation of SUSY quantities.

$$(\bar{\sigma}^m)^{\dot{\alpha}\alpha} \xi_\alpha$$

$$(\bar{\sigma}^m)_{\dot{\beta}}^{\alpha} \xi_\alpha$$

Figure 8: Partially contracted cases. $(\bar{\sigma}^m)^{\dot{\alpha}\alpha} \xi_\alpha$ and $(\bar{\sigma}^m)_{\dot{\beta}}^{\alpha} \xi_\alpha$.

Figure 9: A graphical formula. $= -$ and $= -$.

Some demonstrations will be given later. We express the formula: $=$
 $= -$, $- = -$, $- = -$ in Fig.9. The last equalities in the both lines of the figure comes from the anti-commutability of the spinor graphs (GR 2). We can express all formulae graphically. In this subsection, we list only basic ones. In Fig.10, the symmetric combination of $\bar{\sigma}^m$ are shown as the basic spinor algebra. The antisymmetric combination gives the generators of the Lorentz group, $\bar{\sigma}^{nm}$; $\bar{\sigma}^{nm}$.

$$(\bar{\sigma}^{nm}) = \frac{1}{4} \left(\begin{array}{c} \text{Diagram with } \sigma^n \text{ and } \bar{\sigma}^m \\ \text{Index alpha on left, beta on right} \end{array} \right) \quad m \neq n ;$$

$$(\bar{\sigma}^{nm})^- = \frac{1}{4} \left(\begin{array}{c} \text{Diagram with } \bar{\sigma}^n \text{ and } \sigma^m \\ \text{Index alpha on left, beta on right} \end{array} \right) \quad m \neq n ; \quad (2)$$

Although we have already used $\bar{\sigma}^m$, its definition in terms of $\bar{\sigma}^m$ and the "inverse" relation are displayed in Fig.11. Here we do the upward and downward changes, within the $\bar{\sigma}^m$ and σ^m , by $\bar{\sigma}^n$ and σ^n as explained for the spinor in (1). Using the relation Fig.11, we can obtain the following useful relation.

Graphical Formula: Figure 11B

$$\begin{array}{c}
 \text{Diagram 1:} \\
 \text{Two wavy lines labeled } \sigma^m \text{ and } \bar{\sigma}^n \text{ meet at a vertex.} \\
 \text{The left line } \sigma^m \text{ has a label } \dot{\alpha} \text{ at its left end.} \\
 \text{The right line } \bar{\sigma}^n \text{ has a label } \dot{\beta} \text{ at its right end.} \\
 \text{The two lines are connected by a dashed line labeled } m \text{ and } n \text{ with a double-headed arrow.} \\
 \text{Equation: } m \longleftrightarrow n = -2\eta^{mn} \delta_{\dot{\beta}}^{\dot{\alpha}}
 \end{array}$$

$$\begin{array}{c}
 \text{Diagram 2:} \\
 \text{Two wavy lines labeled } \sigma^m \text{ and } \bar{\sigma}^n \text{ meet at a vertex.} \\
 \text{The left line } \sigma^m \text{ has a label } \alpha \text{ at its left end.} \\
 \text{The right line } \bar{\sigma}^n \text{ has a label } \beta \text{ at its right end.} \\
 \text{The two lines are connected by a dashed line labeled } m \text{ and } n \text{ with a double-headed arrow.} \\
 \text{Equation: } m \longleftrightarrow n = -2\eta^{mn} \delta_{\alpha}^{\beta}
 \end{array}$$

Figure 10: A graphical formula of the basic spinor algebra. $(^m) - (^n) \perp + m \otimes n = 2^{m-n} \perp$, and $(^m) \perp (^n) - + m \otimes n = 2^{m-n} \perp$.

$$\begin{array}{ccc}
 \begin{array}{c} \text{---} \\ \text{---} \\ \text{---} \end{array} & = & \begin{array}{c} \text{---} \\ \text{---} \\ \text{---} \end{array} \\
 \begin{array}{c} \text{---} \\ \text{---} \\ \text{---} \end{array} & = & \begin{array}{c} \text{---} \\ \text{---} \\ \text{---} \end{array}
 \end{array}$$

Figure 11: Definition of m , $(m)^-$, $(m)^{--}$, and its "inverse" relation, $(m)^- = - (m)^{--}$.

$$\begin{array}{c} \sigma^a \quad \bar{\sigma}^b \quad \sigma^c \\ \swarrow \quad \searrow \quad \swarrow \quad \searrow \\ \alpha \quad \dot{\alpha} \quad \alpha \quad \dot{\alpha} \end{array} = \eta^{ac} \begin{array}{c} \sigma^b \\ \swarrow \quad \searrow \\ \alpha \quad \dot{\alpha} \end{array} - \eta^{bc} \begin{array}{c} \sigma^a \\ \swarrow \quad \searrow \\ \alpha \quad \dot{\alpha} \end{array} - \eta^{ab} \begin{array}{c} \sigma^c \\ \swarrow \quad \searrow \\ \alpha \quad \dot{\alpha} \end{array} + i \varepsilon^{abcd} \begin{array}{c} \sigma_d \\ \swarrow \quad \searrow \\ \alpha \quad \dot{\alpha} \end{array}$$

$$\begin{array}{c} \bar{\sigma}^a \quad \sigma^b \quad \bar{\sigma}^c \\ \swarrow \quad \searrow \quad \swarrow \quad \searrow \\ \dot{\alpha} \quad \alpha \quad \dot{\alpha} \quad \alpha \end{array} = \eta^{ac} \begin{array}{c} \bar{\sigma}^b \\ \swarrow \quad \searrow \\ \dot{\alpha} \quad \alpha \end{array} - \eta^{bc} \begin{array}{c} \bar{\sigma}^a \\ \swarrow \quad \searrow \\ \dot{\alpha} \quad \alpha \end{array} - \eta^{ab} \begin{array}{c} \bar{\sigma}^c \\ \swarrow \quad \searrow \\ \dot{\alpha} \quad \alpha \end{array} - i \varepsilon^{abcd} \begin{array}{c} \bar{\sigma}_d \\ \swarrow \quad \searrow \\ \dot{\alpha} \quad \alpha \end{array}$$

Figure 12: Two relations: 1) $\begin{array}{c} a \quad b \quad c \\ \swarrow \quad \searrow \quad \swarrow \quad \searrow \\ \alpha \quad \dot{\alpha} \quad \alpha \quad \dot{\alpha} \end{array} = \begin{array}{c} a \quad c \quad b \\ \swarrow \quad \searrow \quad \swarrow \quad \searrow \\ \alpha \quad \dot{\alpha} \quad \alpha \quad \dot{\alpha} \end{array} + i \varepsilon^{abcd} \begin{array}{c} \sigma_d \\ \swarrow \quad \searrow \\ \alpha \quad \dot{\alpha} \end{array}$, 2) $\begin{array}{c} a \quad b \quad c \\ \swarrow \quad \searrow \quad \swarrow \quad \searrow \\ \alpha \quad \dot{\alpha} \quad \alpha \quad \dot{\alpha} \end{array} = \begin{array}{c} a \quad c \quad b \\ \swarrow \quad \searrow \quad \swarrow \quad \searrow \\ \dot{\alpha} \quad \alpha \quad \dot{\alpha} \quad \alpha \end{array} + i \varepsilon^{abcd} \begin{array}{c} \bar{\sigma}_d \\ \swarrow \quad \searrow \\ \dot{\alpha} \quad \alpha \end{array}$.

$$\delta_{\beta}^{\alpha} \begin{array}{c} \sigma^m \\ \swarrow \quad \searrow \\ \alpha \quad \dot{\alpha} \end{array} \begin{array}{c} \bar{\sigma}^n \\ \swarrow \quad \searrow \\ \beta \quad \dot{\beta} \end{array} = -2 \eta^{mn}$$

$$\begin{array}{c} \sigma^m \\ \swarrow \quad \searrow \\ \alpha \quad \dot{\alpha} \end{array} \begin{array}{c} \bar{\sigma}^n \\ \swarrow \quad \searrow \\ \beta \quad \dot{\beta} \end{array} = -2 \delta_{\alpha}^{\beta} \delta_{\dot{\alpha}}^{\dot{\beta}}$$

Figure 13: Completeness relations: 1) $(\sigma^m)_{-} (\bar{\sigma}^n)_{-} = 2 \delta^{mn}$, 2) $(\sigma^m)_{-} (\bar{\sigma}^n)_{+} = 2 \delta_{-}^{mn}$. The contraction using δ is the matrix trace.

$$\begin{array}{c} \xi \quad \sigma^n \\ \swarrow \quad \searrow \\ \alpha \quad \dot{\alpha} \end{array} \quad \begin{array}{c} \bar{\lambda} \\ \swarrow \quad \searrow \\ \beta \quad \dot{\beta} \end{array} = - \begin{array}{c} \bar{\lambda} \quad \sigma^n \\ \swarrow \quad \searrow \\ \alpha \quad \dot{\alpha} \end{array} \quad \begin{array}{c} \xi \\ \swarrow \quad \searrow \\ \beta \quad \dot{\beta} \end{array} \quad (3)$$

The "reduction" formulae (from the cubic σ^0 's to the linear one) are expressed as in Fig.12. From Fig.12, we notice any chain of σ^0 's can always be expressed by less than three σ^0 's. The appearance of the 4th rank anti-symmetric tensor ε^{abcd} is quite illuminating. The completeness relations are expressed as in Fig.13. The contraction, expressed by δ in Fig.13, is the matrix trace.⁴ Finally we display the Fierz identity.

$$\begin{array}{c} \sigma^n \quad \sigma^m \\ \swarrow \quad \searrow \\ \alpha \quad \beta \end{array} \quad \begin{array}{c} \bar{\sigma}^m \quad \bar{\sigma}^n \\ \swarrow \quad \searrow \\ \beta \quad \dot{\beta} \end{array} = \frac{1}{4} \left(\begin{array}{c} \sigma^n \quad \bar{\sigma}^m \\ \swarrow \quad \searrow \\ \alpha \quad \beta \end{array} - \begin{array}{c} \bar{\sigma}^n \quad \sigma^m \\ \swarrow \quad \searrow \\ \beta \quad \dot{\beta} \end{array} \right) + \left(\begin{array}{c} \bar{\sigma}^n \quad \sigma^m \\ \swarrow \quad \searrow \\ \alpha \quad \beta \end{array} - \begin{array}{c} \sigma^l \quad \bar{\sigma}^n \\ \swarrow \quad \searrow \\ \alpha \quad \beta \end{array} \right) \left(\begin{array}{c} \bar{\sigma}^l \quad \sigma^m \\ \swarrow \quad \searrow \\ \alpha \quad \beta \end{array} - \begin{array}{c} \sigma^l \quad \bar{\sigma}^m \\ \swarrow \quad \searrow \\ \alpha \quad \beta \end{array} \right) \quad (4)$$

⁴We do not, at present, the matrix trace graphical.

where the relation: $(^n) \perp (^m) \perp = 2 (^{ln}) \perp (^{lm}) \perp$, is expressed.

3 4D Chiral Multiplet

As the first example, we take the 4D chiral multiplet. It is made of a complex scalar field A , a Weyl spinor ψ and an auxiliary field (complex scalar) F . Their transformations are expressed as follows.

$$\begin{aligned}
 A &= \frac{p}{2} \xi \perp \psi \quad ; \\
 &= i \frac{p}{2} \xi^m \perp \partial_m A + \frac{p}{2} \xi \perp F = i \frac{p}{2} \xi^m \perp \sigma^m \xi \perp \partial_m A + \frac{p}{2} \xi^m \perp \sigma^m \xi \perp F \quad ; \\
 F &= i \frac{p}{2} \xi^m \perp ({}^m) \perp \partial_m = i \frac{p}{2} \xi^m \perp \bar{\sigma}^n \xi \perp \bar{\psi} \quad : (5)
 \end{aligned}$$

The complex conjugate ones are given as

$$\begin{aligned}
 A &= \frac{p}{2} \xi \perp \bar{\psi} \quad ; \\
 &= i \frac{p}{2} ({}^m) \perp \partial_m A + \frac{p}{2} ({}^m) \perp F = i \frac{p}{2} \xi^m \perp \bar{\sigma}^n \xi \perp \partial_m A + \frac{p}{2} \xi^m \perp \bar{\sigma}^n \xi \perp F \quad ; \\
 F &= i \frac{p}{2} ({}^m) \perp \partial_m = i \frac{p}{2} \xi^m \perp \bar{\sigma}^n \xi \perp \bar{\psi} \quad : (6)
 \end{aligned}$$

We can read the graphical rule of the complex conjugate operation by comparing (5) and (6).

Graphical Rule 6: Complex Conjugation Operation

$$\begin{array}{ccc}
 \xi \perp \psi & ! & \xi \perp \bar{\psi} \quad ; \\
 \bar{\xi} \perp \bar{\psi} & ! & \bar{\xi} \perp \bar{\psi} \quad : \quad (7)
 \end{array}$$

In order to show the graphical representation, presented in Sec.2, satisfies the SUSY representation and the usage of the graphical rules and formulae, we graphically show the SUSY symmetry of the Lagrangian.

$$L = i \partial_n \perp ({}^n) \perp + A \perp 2 A + F \perp F \quad ;$$

$$= \text{ i } \bar{\psi} \text{ } \overset{\circ}{\sigma} \text{ } \psi + A \text{ } 2A + F \text{ } F \quad ; \quad (8)$$

(Hermicity of the first term, up to a total derivative, can be confirmed by the use of GR6 and Fig. 11B.) The three terms in the Lagrangian transform as

$\langle 1 \rangle + \langle 1^0 \rangle = 0$ can be shown as

$$\begin{aligned}
 & <1> = i^p \frac{1}{2} \bar{\sigma}_n \quad \bar{\sigma}^n \quad \xi \quad ! \quad F \\
 & = i^p \frac{1}{2} \bar{\sigma}_n \quad \xi \quad \bar{\sigma}^n \quad \bar{\psi} \quad ! \quad F = <1^0> ; \quad (10)
 \end{aligned}$$

where graph formula Fig.11B is used. $\langle 2 \rangle + \langle 2^0 \rangle =$ a total derivative is shown as

$$\begin{aligned}
 <2> &= \frac{p}{2} \bar{\psi} \begin{array}{c} \nearrow \sigma^n \\ \searrow \bar{\sigma}^n \end{array} \begin{array}{c} \nearrow \sigma^m \\ \searrow \bar{\xi} \end{array} \mathcal{G}_m A = \\
 & \quad ! \\
 & \frac{p}{2} \bar{\psi} \begin{array}{c} \nearrow \bar{\sigma}^n \\ \searrow \sigma^n \end{array} \begin{array}{c} \nearrow \bar{\xi} \\ \searrow \sigma^m \end{array} \mathcal{G}_m A \\
 & + \frac{p}{2} \bar{\psi} \begin{array}{c} \nearrow \bar{\sigma}^n \\ \searrow \sigma^n \end{array} \begin{array}{c} \nearrow \sigma^m \\ \searrow \bar{\xi} \end{array} \mathcal{G}_n \mathcal{G}_m A = \\
 & \quad \varnothing \quad \frac{p}{2} \bar{\xi} \begin{array}{c} \nearrow \bar{\psi} \\ \searrow \psi \end{array} 2A = \varnothing \quad <2^0> \quad ; \quad (11)
 \end{aligned}$$

where " \mathcal{O} " means the corresponding previous graph. In the above the relations Fig.10 and Fig.9 are used. $\langle 4 \rangle + \langle 4^0 \rangle =$ a total derivative can be shown as

$$\begin{aligned}
 \langle 4 \rangle &= \frac{p}{2} \bar{\sigma}^m \swarrow \xi \mathcal{O}_n \mathcal{O}_m A \swarrow \bar{\sigma}^n \psi \\
 &= \frac{p}{2} \xi \swarrow \sigma^m \swarrow \bar{\sigma}^n \psi \mathcal{O}_n \mathcal{O}_m A \\
 &= \frac{p}{2} \xi \swarrow \psi 2A ; \\
 \langle 4^0 \rangle &= \mathcal{O}_n \left(\frac{p}{2A} \xi \swarrow \psi \right) \frac{p}{2\mathcal{O}^n A} \xi \swarrow \psi \\
 &\quad + \frac{p}{2} \xi \swarrow \psi 2A ; \quad (12)
 \end{aligned}$$

where some modification of Fig.11B is used in the first line, and Fig.10 is used in the second line. $\langle 3 \rangle + \langle 3^0 \rangle =$ a total derivative can be obtained as

$$\langle 3 \rangle = i \frac{p}{2\mathcal{O}_n} F \xi \swarrow \bar{\sigma}^n \swarrow \psi ! \frac{p}{2F} \xi \swarrow \bar{\sigma}^n \swarrow \psi = \mathcal{O} \quad \langle 3^0 \rangle : (13)$$

Summing the above results, we finally obtain the result.

$$\begin{aligned}
 L &= \mathcal{O}_n \left(\frac{p}{2} \bar{\psi} \swarrow \bar{\sigma}^n \swarrow \sigma^m \swarrow \xi \mathcal{O}_m A + \frac{p}{2A} \mathcal{O}^n \left(\xi \swarrow \psi \right) \right) \\
 &\quad + \frac{p}{2\mathcal{O}^n A} \xi \swarrow \psi + i \frac{p}{2F} \xi \swarrow \bar{\sigma}^n \swarrow \psi : (14)
 \end{aligned}$$

Hence the Lagrangian indeed invariant up to a total derivative.

4 4D Vector Multiplet

The superelectromagnetic theory, in the WZ gauge, is given by

$$L_{EM} = \frac{1}{2} D^2 - \frac{1}{4} v_m^n v_{m n} - i \lambda \swarrow \bar{\sigma} \swarrow \lambda ; \quad (15)$$

where $v_{m n} = \mathcal{O}_m v_n - \mathcal{O}_n v_m$. v_m is the vector field, λ is the Weyl fermion, D is a scalar auxiliary field. (15) is invariant under the SUSY transformation.

$$D = \lambda \swarrow \bar{\sigma} \swarrow \lambda - \xi \swarrow \bar{\sigma} \swarrow \lambda ; \quad$$



Figure 14: The graphical representation for the Majorana spinor, $\bar{\Psi}_S$, and its conjugate Ψ_S . $s = 1, 2, 3, 4$:

$$\begin{aligned}
 \alpha \not{\lambda} &= i \not{\xi} D + \frac{1}{4} \not{\alpha} \not{\sigma}^m \not{\bar{\sigma}}^n \not{\xi} \quad m \neq n \quad v_{mn} ; \\
 v_{mn} &= i \not{\xi} \not{\sigma}^n \not{\bar{\sigma}}^m \not{\lambda} + i \not{\xi} \not{\sigma}^n \not{\bar{\sigma}}^m \not{\lambda} \quad m \neq n ; \\
 v_m &= i \not{\xi} \not{\sigma}^m \not{\bar{\lambda}} + i \not{\xi} \not{\sigma}^m \not{\bar{\sigma}}^m \not{\lambda} \quad ; \quad (16)
 \end{aligned}$$

The SUSY invariance of (15) can be graphically shown by using the relations of Fig.9, Fig.11, Fig.12 and Fig.11B. The result is

$$\begin{aligned}
 L_E M &= \partial_1 - \not{\lambda} \not{\sigma}^1 \not{\xi} D - i \not{\lambda} \not{\sigma}^m \not{\xi} v_{m1} \\
 &\quad + \frac{1}{2} \epsilon^{lmns} \not{\bar{\lambda}} \not{\bar{\sigma}}_s \not{\xi} v_{mn} \quad ; \quad (17)
 \end{aligned}$$

which express a total derivative. The appearance of the totally anti-symmetric tensor ϵ^{lmns} shows that the invariance depends on the space-time dimensionality 4 in the case of vector multiplet.

5 Majorana spinor

Another useful way to represent the supersymmetry is the use of the Majorana spinor which is based on $SO(1,3)$ (not $SL(2, \mathbb{C})$) structure. We define the graphical representation for the Majorana spinor and its conjugate Ψ_S as in Fig.14. The $SO(1,3)$ invariants and ϵ^5 are represented as in Fig.15. They are graphically much simpler than the Weyl case (no arrows, the single (vertical) wedge structure with spinor matrices placed at the vertex) because only the adjoint structure is necessary to be build in the graph. Remaining information, such as hermiticity and chiral properties, is in the 4×4 matrix elements (made of 4×4 matrices).

The relation between the Weyl and Majorana spinors is described in textbooks [5, 6, 7]. To show the precise relation, at the graphical level, and to show some

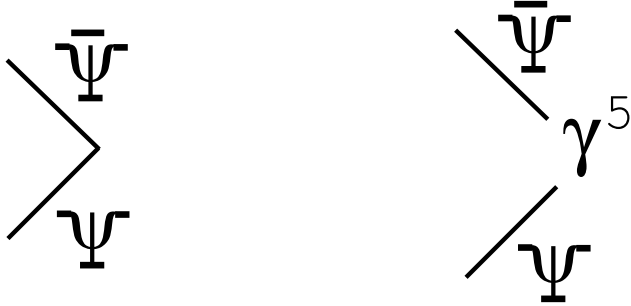


Figure 15: The graphical representation for the $SO(1,3)$ invariants made of the Majorana spinors: ψ and $\bar{\psi}$.

usage of the graph method, we derive the relation using the previously defined contents. The chiral multiplet of Sec.3 is taken for the explanation.

First we introduce 4 real fields $P; Q; G; H$, instead of $(A; A'; F; F')$.

$$\begin{aligned} P &= \frac{1}{2} (A + A') & Q &= \frac{1}{2i} (A - A') \\ G &= \frac{1}{2} (F + F') & H &= \frac{1}{2i} (F - F') \end{aligned} \quad (18)$$

As for spinor quantities, we introduce 4 components spinor quantities $\psi, \bar{\psi}, \xi, \bar{\xi}$ instead of the 2 components ones $(\psi, \bar{\psi}, \xi, \bar{\xi})$.

$$\begin{aligned} &= \psi \quad ; \quad = \bar{\psi} \quad ; \\ &= \xi \quad ; \quad = \bar{\xi} \quad : \end{aligned} \quad (19)$$

Using these quantities the SUSY transformation (of the chiral multiplet) is obtained as

$$\begin{aligned} & P = \psi + \bar{\psi} = \bar{\alpha} \quad ; \\ & Q = \frac{1}{i} (\psi - \bar{\psi}) = \gamma^5 \quad ; \\ & G = i \psi - \bar{\xi} + i \bar{\psi} - \xi = i \gamma^m \xi \quad ; \\ & H = i \bar{\psi} \bar{\sigma} + i \psi \sigma = i \gamma^m \bar{\xi} \quad ; \end{aligned}$$

$$\begin{aligned}
H &= \underline{(\underline{m})} - \underline{\theta_m} & (\underline{m}) \underline{\theta_m} &= i \underline{\gamma^5 m \theta_m} \\
&= \begin{array}{c} \text{Diagram with } \bar{\sigma} \text{ loop, } 0 \text{ below} \end{array} & \begin{array}{c} \text{Diagram with } \sigma \text{ loop, } 1 \text{ below} \end{array} & ; \\
&= \begin{array}{c} \text{Diagram with } \bar{\sigma} \text{ loop, } 0 \text{ below} \end{array} - \begin{array}{c} \text{Diagram with } \bar{\sigma} \text{ loop, } 0 \text{ below} \end{array} = \begin{array}{c} \text{Diagram with } \bar{\sigma} \text{ loop, } 0 \text{ below} \end{array} + \begin{array}{c} \text{Diagram with } \sigma \text{ loop, } 1 \text{ below} \end{array} \\
&= \begin{array}{c} \text{Diagram with } \bar{\sigma} \text{ loop, } 0 \text{ below} \end{array} + \begin{array}{c} \text{Diagram with } \sigma \text{ loop, } 1 \text{ below} \end{array} \\
&= i \underline{\theta_m (P - \gamma^5 Q)^m} + (G - \gamma^5 H) \\
&= i \underline{\theta_m (P - \gamma^5 Q)^m} + \underline{(G - \gamma^5 H)} & ; & (20)
\end{aligned}$$

where the double lines are used to express the SUSY parameters and the following gamma matrices are taken:

$$\underline{m} = \begin{array}{cc} 0 & (\underline{m}) \\ (\underline{m}) & 0 \end{array} ; \quad \underline{5} = \begin{array}{cccc} 0 & 1 & 2 & 3 \end{array} = \begin{array}{cc} i & 0 \\ 0 & i \end{array} ; \quad (21)$$

We show here the graphical expressions for the SO(1,3) invariants made of the Majorana spinors: $i \underline{\theta_m}$; $i \underline{\gamma^5 m \theta_m}$; $i \underline{\theta_m (P - \gamma^5 Q)^m}$; $(G - \gamma^5 H)$. The above graphical relations manifestly show the $\underline{5}$ matrix controls the chirality in the Majorana spinor, whereas it is shown by the left-right direction (dot-undotted axes) in the Weyl case. The above relations can be used in the transformation between both expressions even at the graphical level.

The fermion kinetic term of the chiral Lagrangian (8) is graphically transformed into the Majorana expression as follows.

$$\begin{aligned}
& \begin{array}{c} \text{Diagram with } \bar{\sigma} \text{ loop, } 0 \text{ below} \end{array} = \frac{i}{2} \begin{array}{c} \text{Diagram with } \bar{\sigma} \text{ loop, } 0 \text{ below} \end{array} & \begin{array}{c} \text{Diagram with } \bar{\sigma} \text{ loop, } 0 \text{ below} \end{array} \\
& = \frac{i}{2} \underline{\theta_m} \begin{array}{c} \text{Diagram with } \bar{\sigma} \text{ loop, } 0 \text{ below} \end{array} & ! \quad \begin{array}{c} \text{Diagram with } \bar{\sigma} \text{ loop, } 0 \text{ below} \end{array} \\
& = \frac{i}{2} \underline{\theta_m} (\underline{\infty}) \quad \frac{i}{2} - \begin{array}{c} \text{Diagram with } \bar{\sigma} \text{ loop, } 0 \text{ below} \end{array} - \begin{array}{c} \text{Diagram with } \bar{\sigma} \text{ loop, } 0 \text{ below} \end{array} - \underline{\theta_m} \\
& = \frac{i}{2} \underline{\theta_m} (\underline{\infty}) \quad \frac{i}{2} \underline{m \theta_m} = \frac{i}{2} \underline{\theta_m} (\underline{\infty}) \quad \frac{i}{2} \underline{\gamma^5 m \theta_m} & ; & (22)
\end{aligned}$$

where the relation of Fig.11B is used in the first line.

6 Indices of Graph

We introduce some indices of a graph. They classify graphs. Its use is another advantage of the graphical representation.

(i) Left Chiral Number and Right Chiral Number

We assign $\frac{1}{2}$ for each one step leftward arrow and define its total sum within a graph as Left Chiral Number (LCN). In the same way, we assign $\frac{1}{2}$ for each one step rightward arrow and define its total sum within a graph as Right Chiral Number (RCN).

(ii) Up-Down Counting

We assign $+\frac{1}{2}$ for one step of the upward arrow and $-\frac{1}{2}$ for the one step of the downward arrow. Then we define Left Up-Down Number (LUDN) as the total sum for all leftward arrow within a graph, and Right Up-Down Number (RUDN) as the total sum for all rightward arrow within a graph. For $SL(2, \mathbb{C})$ invariants, these indices vanish.

In order to count the number of the \times contraction we introduce the following ones.

(iii) Left W edge Number and Right W edge Number

We assign 1 for each piece of  and define the total sum within a graph as Left W edge Number (LWN). In the same way, we assign 1 for each piece of  and define the total sum within a graph as Right W edge Number (RWN).

(iv) Dotted Line Number

We assign 1 for one dotted line which connects the space-time \times . We define the total sum within a graph as Dotted Line Number (DLN).

In addition to the graph-related indices, we introduce

a) Physical Dimension (DIM); b) Number of the derivatives (DF); c) Number of σ (SIG)

We list the above indices for basic spinor quantities in Table 1 and for the operators appearing the chiral multiplet Lagrangian (Sec.3) in Table 2.

| | ψ | $\bar{\psi}$ | σ^m | $\bar{\sigma}^m$ |
|--------------|---------------------|---------------------|--------------------------------|------------------------------|
| (LCN, RCN) | $(\frac{1}{2}; 0)$ | $(0; \frac{1}{2})$ | $(\frac{1}{2}; \frac{1}{2})$ | $(\frac{1}{2}; \frac{1}{2})$ |
| (LUDN, RUDN) | $(-\frac{1}{2}; 0)$ | $(0; +\frac{1}{2})$ | $(-\frac{1}{2}; -\frac{1}{2})$ | $(\frac{1}{2}; \frac{1}{2})$ |
| (LWN, RWN) | 0 | 0 | 0 | 0 |
| DLN | 0 | 0 | 0 | 0 |
| DIM | $\frac{3}{2}$ | $\frac{3}{2}$ | 0 | 0 |
| DF | 0 | 0 | 0 | 0 |
| SIG | 0 | 0 | 1 | 1 |

Table 1 Indices for basic spinor quantities: ψ ; $\bar{\psi}$; σ^m ; $\bar{\sigma}^m$.

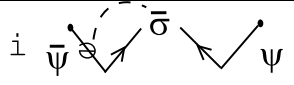
| |  | A 2 A | F F |
|--------------|---|-------|-----|
| (LCN, RCN) | (1;1) | / | / |
| (LUDN, RUDN) | (0;0) | / | / |
| (LWN, RW D) | (1,1) | / | / |
| D LN | 1 | / | / |
| D IM | 4 | 4 | 4 |
| D IF | 1 | 2 | 0 |
| SIG | 1 | 0 | 0 |

Table 2 Indices for operators appearing in the chiral multiplet Lagrangian. We can identify every term appearing in the theory in terms of some of these indices. We list some indices for all spinorial operators in Super QED. We see

all terms are classified by the indices and the field contents.

| | | (LCN, RCN) = (LWN, RWN) | $(LUDN, RUDN)$ | DF | Fields |
|----|--|--------------------------------|----------------|----|-------------------|
| 1 | | (1;1) | (0;0) | 1 | ; |
| 2 | | (1;1) | (0;0) | 1 | $+$; $+$ |
| 3 | | (1;1) | (0;0) | 1 | ; |
| 4 | | (1;1) | (0;0) | 0 | $+$; $+$; v^m |
| 5 | | (1;1) | (0;0) | 0 | ; v^m |
| 6 | | (0;1) | (0;0) | 0 | A_+ ; $+$; |
| 7 | | (0;1) | (0;0) | 0 | A ; ; |
| 8 | | (1;0) | (0;0) | 0 | A_+ ; $+$; |
| 9 | | (1;0) | (0;0) | 0 | A ; ; |
| 10 | | (1;0) | (0;0) | 0 | $+$; |
| 11 | | (0;1) | (0;0) | 0 | $+$; |

Table 3 List of indices for all spinor operators in the super QED Lagrangian.
 $(;)$: photino; v^m : photon; $(+ ; +)$: + chiral fermion; $(; -)$: - chiral fermion.

7 Superspace Quantities

We know the SUSY symmetry is most naturally viewed in the superspace $(x^m; ;)$. Here we introduce anti-commuting parameters $= ; ; - ; -$ as the basic spinor coordinate. We show them graphically in Fig.16. They satisfy the graphical relations of Fig.17.

The general super field $F(x; ;)$, in terms of components fields

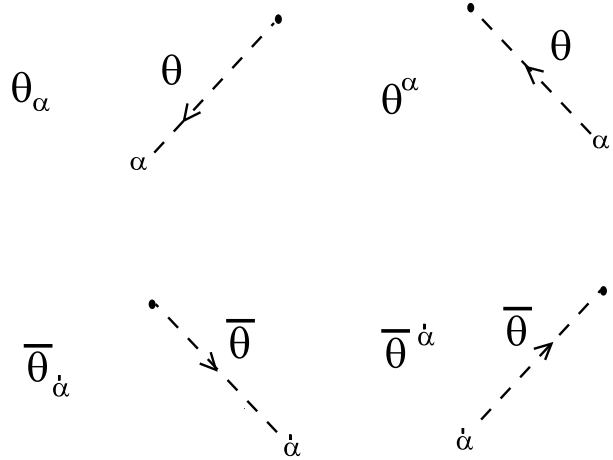


Figure 16: The graphical representation for the spinor coordinates in the superspace: $+$, $-$, $_$ and $_$.

$$\begin{aligned}
 \theta^{\dot{\alpha}}_{\dot{\beta}} \theta^{\dot{\gamma}}_{\dot{\delta}} &= -\frac{1}{2} \varepsilon^{\alpha\beta} \theta^{\dot{\gamma}}_{\dot{\beta}} \theta^{\dot{\delta}}_{\dot{\alpha}} \\
 \theta^{\dot{\alpha}}_{\dot{\beta}} \theta^{\dot{\gamma}}_{\dot{\delta}} &= \frac{1}{2} \varepsilon_{\alpha\beta} \theta^{\dot{\gamma}}_{\dot{\beta}} \theta^{\dot{\delta}}_{\dot{\alpha}} \\
 \bar{\theta}^{\dot{\alpha}}_{\dot{\beta}} \bar{\theta}^{\dot{\gamma}}_{\dot{\delta}} &= \frac{1}{2} \varepsilon^{\dot{\alpha}\dot{\beta}} \bar{\theta}^{\dot{\gamma}}_{\dot{\beta}} \bar{\theta}^{\dot{\delta}}_{\dot{\alpha}} \\
 \bar{\theta}^{\dot{\alpha}}_{\dot{\beta}} \bar{\theta}^{\dot{\gamma}}_{\dot{\delta}} &= -\frac{1}{2} \varepsilon_{\dot{\alpha}\dot{\beta}} \bar{\theta}^{\dot{\gamma}}_{\dot{\beta}} \bar{\theta}^{\dot{\delta}}_{\dot{\alpha}}
 \end{aligned}$$

Figure 17: The graphical rules for the spinor coordinates:

($\phi(x)$; $\chi(x)$; $m(x)$; $n(x)$; $v_m(x)$; $d(x)$), is shown as

$$F(x; \theta) = f(x) + \sqrt{\theta} \phi(x) + \sqrt{\theta} \chi(x) + \sqrt{\theta} m(x) + \sqrt{\theta} n(x) + \sqrt{\theta} v_m(x) + \sqrt{\theta} \lambda(x) + \sqrt{\theta} \psi(x) + \sqrt{\theta} d(x) \quad : (23)$$

The SUSY transformation generator Q and Q_- are expressed as

$$Q = \frac{\theta}{\theta} + i \begin{array}{c} \sigma \\ \diagup \quad \diagdown \\ \alpha \quad \bar{\alpha} \end{array} \quad ;$$

$$Q_- = \frac{\theta_-}{\theta} + i \begin{array}{c} \sigma \\ \diagup \quad \diagdown \\ \bar{\alpha} \quad \alpha \end{array} \quad ; \quad (24)$$

The SUSY derivative operators D and D_- , which are the conjugate partners of Q and Q_- , are expressed as

$$D = \frac{\theta}{\theta} + i \begin{array}{c} \sigma \\ \diagup \quad \diagdown \\ \alpha \quad \bar{\alpha} \end{array} \quad ;$$

$$D_- = \frac{\theta_-}{\theta} - i \begin{array}{c} \sigma \\ \diagup \quad \diagdown \\ \bar{\alpha} \quad \alpha \end{array} \quad ; \quad (25)$$

We can graphically confirm the SUSY algebra by using the commutativity and anti-commutativity between Q ; Q_- ; D ; D_- and θ .

$$fQ \cdot Q_- g = 2i \begin{array}{c} \sigma \\ \diagup \quad \diagdown \\ \alpha \quad \bar{\alpha} \end{array} \quad ;$$

$$fD \cdot D_- g = -2i \begin{array}{c} \sigma \\ \diagup \quad \diagdown \\ \bar{\alpha} \quad \alpha \end{array} \quad ; \quad (26)$$

In the treatment of the chiral supereld, it is important to choose appropriate coordinates: ($y^m = x^m + i \theta^m$; $\bar{y}^m = \bar{x}^m - i \bar{\theta}^m$) for the chiral eld, and ($y^{ym} = x^m$; $\bar{y}^{ym} = \bar{x}^m$) for the anti-chiral one.

$$y^m = x^m + i \theta^m \quad ;$$

$$y^{ym} = x^m - i \bar{\theta}^m \quad ; \quad (27)$$

Because of the properties $D_- y^m = 0; D_+ = 0$ and $D_- y^{\bar{m}} = 0; D_+ = 0$, the chiral supereld $(D_- = 0)$ and the anti-chiral one $(D_+ = 0)$ are always written as

$$(y; \bar{y}; \theta) = A(y) + \frac{p}{2} \bar{\theta} \not{\partial} \psi(y) + \not{\partial} \bar{\psi}(y^+) F(y);$$

and

$${}^y(y^y; \bar{y}; \theta) = A(y^y) + \frac{p}{2} \bar{\theta} \not{\partial} \psi(y^+) + \not{\partial} \bar{\psi}(y^+) F(y^y); \quad (28)$$

respectively. The SUSY differential operators are expressed as, in terms of $(y; \bar{y}; \theta)$,

$$D_+ = \frac{\theta}{\theta} + 2i \not{\partial} \bar{\psi} \not{\partial} \psi \not{\partial} \bar{\theta} \bar{\partial}_y; \quad D_- = \frac{\theta}{\theta_-};$$

$$Q_+ = \frac{\theta}{\theta} \not{\partial} \bar{\psi} \not{\partial} \psi \not{\partial} \bar{\theta} \bar{\partial}_y; \quad Q_- = \frac{\theta}{\theta_-} + 2i \not{\partial} \bar{\psi} \not{\partial} \psi \not{\partial} \bar{\theta} \bar{\partial}_y; \quad (29)$$

and as, in terms of $(y^y; \bar{y}; \theta)$,

$$D_+ = \frac{\theta}{\theta} \not{\partial} \bar{\psi} \not{\partial} \psi \not{\partial} \bar{\theta} \bar{\partial}_{y^+};$$

$$Q_+ = \frac{\theta}{\theta} \not{\partial} \bar{\psi} \not{\partial} \psi \not{\partial} \bar{\theta} \bar{\partial}_{y^+}; \quad Q_- = \frac{\theta}{\theta_-} \not{\partial} \bar{\psi} \not{\partial} \psi \not{\partial} \bar{\theta} \bar{\partial}_{y^+}; \quad (30)$$

The superspace calculation can be performed graphically. For example, the y^y calculation, in order to find the 4D SUSY Lagrangian, can be done using the graph relations of Fig.17. The advantage, compared to the usual one, is that the graphically expressed quantity is not "obscured" by the dummy (contracted) superspaces.

8 Application to 5D Supersymmetry

In this section we apply the graphical method to a recent subject [8, 9]: 5D supersymmetry. Here both (4-components and 2-components spinors) types of representation appears in relation to SUSY "decomposition". Stimulated by the brane world physics, higher dimensional SUSY becomes an important subject. In particular, 5 dimensional one is used as the concrete extended model of the standard model. The simplest one is the hypermultiplet $(A^i; F^i)$, where both A^i ($i = 1, 2$) and F^i are the $SU(2)_R$ doublet of complex scalars. F^i are the auxiliary fields. A^i is a Dirac field. The $SU(2)_R$ index, i , is lowered or raised by ${}_{ij}$ and ${}^{ij}: A_i = {}_{ij} A^j; F^i = {}^{ij} F_j$ where ${}_{ij}$ and ij are the same as (1).

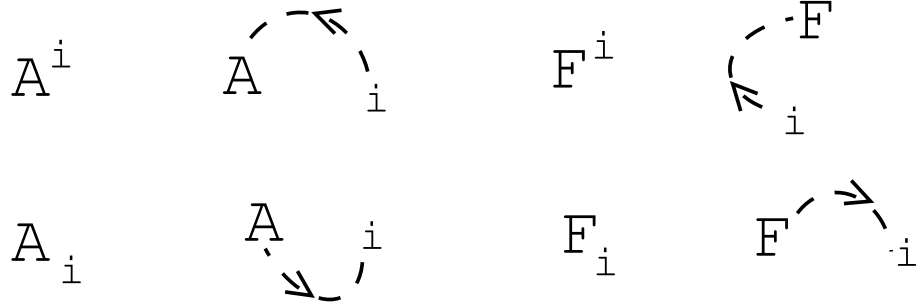


Figure 18: The graphical representation for the $SU(2)_R$ doublet fields, $A^i; A_i = \epsilon_{ij}A^j; F_i$ and $F^i = \epsilon^{ij}F_j$. The arrowed dotted line is depicted arbitrarily except that the one end should be attached to the symbol and the correct arrow direction should be taken.

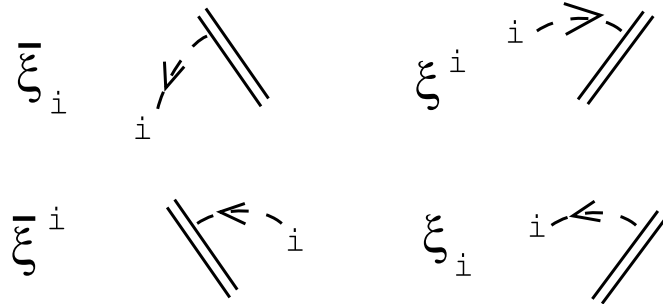


Figure 19: The graphical representation for the 5D SUSY parameters, ξ_i^i and ξ_i^i .

The doublet fields are graphically represented as in Fig.18. The $su(2)$ up-down is expressed by the arrow direction: the out-in direction for the up- $su(2)$ and the in-out direction for the down- $su(2)$. (This representation of the $su(2)$ up-down is different from the treatment taken in the spinor case of Sec.2.)

As the 5D SUSY parameter, we take the symplectic Majorana spinors. They are $SU(2)_R$ doublet of Dirac spinors ($i = 1, 2$) which satisfy the symplectic Majorana condition ("reality" condition).

$$\xi^i = \epsilon^{ij} C^T_j \quad ; \quad C = \begin{pmatrix} i^2 & 0 \\ 0 & i^2 \end{pmatrix} \quad : \quad (31)$$

From the number of the independent SUSY parameters, we know the present system has 8 (counted in real) supercharges. We introduce the graphical representation for ξ^i and ξ_i^i as in Fig.19. The Dirac spinor structure is graphically the same as the Majorana one of Sec.5.

Then the 5D SUSY transformation is expressed as

$$\begin{aligned}
 A^i &= \frac{p}{2} \overline{A}_{ij}^i = \frac{p}{2} \overline{\chi}^i ; \\
 &= \frac{p}{2i} \overline{A}_i^M \theta_M A_{ij}^i + \frac{p}{2} \overline{F}_i^i \\
 &= \frac{p}{2i} \overline{\partial A}^i + \frac{p}{2} \overline{F}^i ; \\
 F_i &= \frac{p}{2i} \overline{A}_i^M \theta_M = \frac{p}{2i} \overline{\chi}^i ; \tag{32}
 \end{aligned}$$

where a wavy line is used to express the 5D space-time supersymmetries ($M = 0, 1, 2, 3, 5$) contraction.⁵ The complex conjugate one is given by

$$\begin{aligned}
 A_i &= \frac{p}{2} \overline{A}_{ij}^i = \frac{p}{2} \overline{\chi}_i ; \\
 &= \frac{p}{2i} \overline{A}_i^M \theta_M A_{ij}^i + \frac{p}{2} \overline{F}_i^i \\
 &= \frac{p}{2i} \overline{\partial A}^i + \frac{p}{2} \overline{F}^i ; \\
 F &= \frac{p}{2i} \overline{A}_i^M \theta_M = \frac{p}{2i} \overline{\chi}_i ; \tag{33}
 \end{aligned}$$

The free Lagrangian is given by

$$\begin{aligned}
 L &= i^M \theta_M \theta^M A_i \theta_M A^i + F^i F_i \\
 &= i \overline{\chi}^i \overline{\partial A}^i + \overline{F}^i \overline{F}^i ; \tag{34}
 \end{aligned}$$

Using the graphical rule of Fig. 20 ($A^i (ij^j) = (jiA^i)^j$), and the basic spinor relation $f^M;^N g = 2^{M^N}$, we can graphically confirm the SUSY invariance.
6

$$\begin{aligned}
 L &= \theta_M \left(\frac{p}{2i} \overline{A}_{ij}^i \overline{\chi}^M \overline{\partial A}^i + \frac{p}{2} \overline{\chi}^i \overline{\partial A}^i \overline{\partial A}^M \right. \\
 &\quad \left. + \frac{p}{2} \overline{F}^i \overline{\partial A}^i \overline{\partial A}^M \right) ; \tag{35}
 \end{aligned}$$

⁵ 5D Dirac gamma matrix is taken to be $(^M) = (^m; ^5)$ where m and 5 are defined in (21).

⁶ $M^N = \text{diag}(1; 1; 1; 1; 1)$

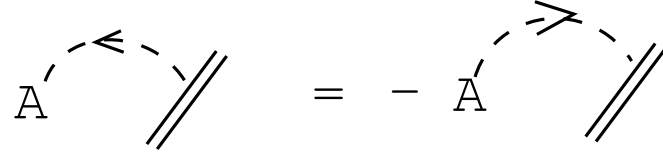


Figure 20: The graphical rules for the relation: $A^i (ij) = - (ji) A^j$.

In relation to the SU SY decomposition, we rewrite the Dirac fields (ψ ; ψ^i ; ψ^i) in terms of Weyl spinors.

$$\begin{aligned}
 &= \begin{array}{c} (L) \\ (R) \end{array} - ; \quad = \begin{array}{c} ((R) ; (L) _) \\ 0 \end{array} ; \\
 &^1 = \begin{array}{c} (1L) \\ (1R) \end{array} - = \begin{array}{c} (1L) \\ (2L) \end{array} - = \begin{array}{c} B \\ \text{---} \\ @ \end{array} ; \quad \begin{array}{c} 1 \\ C \\ A \end{array} ; \\
 &^1 = (1R) ; (1L) _ = (2L) ; (1L) _ = \begin{array}{c} B \\ \text{---} \\ @ \end{array} ; \quad \begin{array}{c} 0 \\ 1 \\ ! \end{array} ; \\
 &^2 = \begin{array}{c} (2L) \\ (2R) \end{array} - = \begin{array}{c} (2L) \\ (1L) \end{array} - = \begin{array}{c} B \\ \text{---} \\ @ \end{array} ; \quad \begin{array}{c} C \\ C \\ A \end{array} ; \\
 &^2 = (2R) ; (2L) _ = (1L) ; (2L) _ = \begin{array}{c} B \\ \text{---} \\ @ \end{array} ; \quad \begin{array}{c} 0 \\ 1 \\ ! \end{array} ; \quad (36)
 \end{aligned}$$

where the reality condition is used to express the SU SY parameters by 8 (counted in real) independent quantities: $_{1L}$, $_{2L}$ and their conjugates. Then the 5D SU SY symmetry (32) is decomposed as follows. For the bosonic part, they are

given by

$$\begin{aligned}
 (1) \quad & \frac{p}{2} \bar{A}^1 = \begin{array}{c} \nearrow \xi_2 \\ \chi \end{array} = \\
 & \begin{array}{c} \xi \\ \nearrow \chi \\ 1L \end{array} \quad : \\
 (2) \quad & \frac{p}{2} \bar{A}^2 = \begin{array}{c} \nearrow \xi_1 \\ \chi \end{array} = \\
 & \begin{array}{c} \xi \\ \nearrow \bar{\chi} \\ 1L \end{array} \quad + \quad \begin{array}{c} \xi \\ \nearrow \chi \\ 2L \end{array} \quad : \\
 (3) \quad & \frac{p}{2i} \bar{F}_1 = \begin{array}{c} \nearrow \xi_1 \\ \chi \end{array} = \\
 & \begin{array}{c} \nearrow \bar{\sigma} \\ \chi \\ L \end{array} + i \begin{array}{c} \nearrow \bar{\sigma} \\ \bar{\chi} \\ R \end{array} + \begin{array}{c} \nearrow \bar{\sigma} \\ \bar{\chi} \\ R \end{array} + i \begin{array}{c} \nearrow \bar{\sigma} \\ \chi \\ L \end{array} \quad : \\
 (4) \quad & \frac{p}{2i} \bar{F}_2 = \begin{array}{c} \nearrow \xi_2 \\ \chi \end{array} = \\
 & \begin{array}{c} \nearrow \bar{\sigma} \\ \bar{\chi} \\ R \end{array} + i \begin{array}{c} \nearrow \bar{\sigma} \\ \chi \\ L \end{array} + \begin{array}{c} \nearrow \bar{\sigma} \\ \chi \\ L \end{array} + i \begin{array}{c} \nearrow \bar{\sigma} \\ \bar{\chi} \\ R \end{array} \quad : \\
 \end{aligned} \tag{37}$$

For the fermionic part they are given by

$$\begin{aligned}
 (6) \quad & \frac{p}{2} \bar{L} = \\
 & i \begin{array}{c} \nearrow \bar{\sigma} \\ \bar{\chi} \end{array} \partial \bar{A}^1 + (\bar{F}_2 + \bar{\Theta}_5 \bar{A}^2) \begin{array}{c} \nearrow \bar{\sigma} \\ \chi \end{array} + i \begin{array}{c} \nearrow \bar{\sigma} \\ \chi \end{array} \partial \bar{A}^2 + (\bar{F}_2 + \bar{\Theta}_5 \bar{A}^1) \begin{array}{c} \nearrow \bar{\sigma} \\ \bar{\chi} \end{array} \quad : \\
 (7) \quad & \frac{p}{2} \bar{R} = \\
 & i \begin{array}{c} \nearrow \bar{\sigma} \\ \bar{\chi} \end{array} \partial \bar{A}^2 + (\bar{F}_2 + \bar{\Theta}_5 \bar{A}^1) \begin{array}{c} \nearrow \bar{\sigma} \\ \bar{\chi} \end{array} + i \begin{array}{c} \nearrow \bar{\sigma} \\ \chi \end{array} \partial \bar{A}^1 + (\bar{F}_1 + \bar{\Theta}_5 \bar{A}^2) \begin{array}{c} \nearrow \bar{\sigma} \\ \chi \end{array} \quad : \\
 \text{where } (5) \quad & \frac{p}{2} = i \begin{array}{c} \nearrow \bar{\sigma} \\ \bar{\chi} \end{array} + \begin{array}{c} \nearrow \bar{\sigma} \\ \chi \end{array} = \begin{array}{c} \nearrow \bar{\sigma} \\ \chi \\ L \end{array} + \begin{array}{c} \nearrow \bar{\sigma} \\ \bar{\chi} \\ R \end{array} \quad : \tag{38}
 \end{aligned}$$

⁷ Let us compare the above result with the decomposition structure in the

⁷ The graph equations in (37) are, in the ordinary expression, as follows.

- (1) $\bar{A}^1 = \frac{p}{2} = \bar{A}_2 = \frac{p}{2} = \bar{A}_1 = \frac{p}{2} = (1L) \bar{A}^1 (L) (2L) \bar{A}^1 (R) ;$
- (2) $\bar{A}^2 = \frac{p}{2} = \bar{A}_2 = \frac{p}{2} = \bar{A}_1 = \frac{p}{2} = 1L \bar{A}^2 R + 2L \bar{A}^2 L ;$
- (3) $\bar{F}_1 = \frac{p}{2i} = \bar{F}^2 = \frac{p}{2i} = 1L \bar{A}^1 m \Theta_m L + i (1L) \bar{A}^1 (2L) \bar{A}^2 R + 2L \bar{A}^1 m \Theta_m R + i (2L) \bar{A}^2 (2L) \bar{A}^1 ;$
- (4) $\bar{F}_2 = \frac{p}{2i} = \bar{F}^1 = \frac{p}{2i} = 1L \bar{A}^2 R + i (1L) \bar{A}^1 (2L) \bar{A}^1 L + 2L \bar{A}^2 m \Theta_m L + i (2L) \bar{A}^1 (2L) \bar{A}^2 ;$
- (5) $\bar{F} = \frac{p}{2} = i^m \Theta_m A^i_{ij} j + F_i^i = (L; R)^T ;$
- (6) $\bar{L} = \frac{p}{2} = i^m 1L \Theta_m A^1 + (\bar{F}_1 + \bar{\Theta}_5 \bar{A}^2) 1L + i^m 2L \Theta_m A^2 + (\bar{F}_2 + \bar{\Theta}_5 \bar{A}^1) 2L ;$
- (7) $\bar{R} = \frac{p}{2} = i^m 1L \Theta_m A^2 + (\bar{F}_2 + \bar{\Theta}_5 \bar{A}^1) 1L + i^m 2L \Theta_m A^1 + (\bar{F}_1 + \bar{\Theta}_5 \bar{A}^2) 2L ;$

case of 4D : M a jprana (4-com ponents) to W eyl (2-com ponents). In the 4D case, the decom position is done w ith respect to chirality (left versus right), and controls it. In the present case of 5D , the decom position is done w ith respect to (1_L ; 1_L) and (2_L ; 2_L), the label1 and 2 control it. Here we note that there is no "chiralm atrix" in 5D in the sense that $M^M / 1$. Next we explain what symmetry plays the role of separation of 1 and 2 .

In relation to the decom position (to $N = 1SUSY$) procedure, we introduce Z_2 -sym m etry, that is the re ection in the origin in the (f th) extra coordinate.

$$x^5 \quad \$ \quad x^5 \quad \vdots \quad (39)$$

We assign the Z_2 -parity to all fields in a consistent way with the decomposition relations (37). A choice is given in Table 4.

| | | |
|-------|---------------------|---------------------|
| | $P = +1 ; \quad 1L$ | $P = -1 ; \quad 2L$ |
| A^1 | A^1 | A^2 |
| | L | R |
| F_i | F_1 | F_2 |

Table 4 Z_2 parity assignment

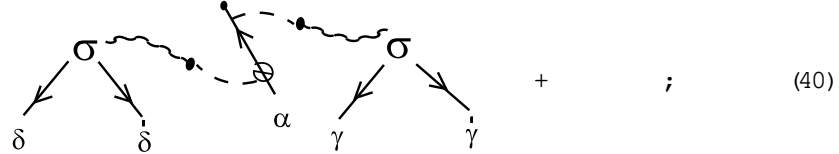
Then the the 5D SU SY symmetry is decomposed to two $N = 1$ chiral multiplets; one is for $P = +1$ states, the other is for $P = -1$ states. Up to now, the SU SY decomposition is not directly related with the space-time dimensional reduction. Let us consider the case that the present 5D SU SY system has the localized configuration around the origin in the extra coordinate. Then we can naturally suppose that the Z_2 -symmetry, which is required from the configuration, restricts the boundary condition of the fields and the whole system decomposes into even-parity and odd-parity fields. Then dimensional reduction occurs.

9 Discussion and conclusion

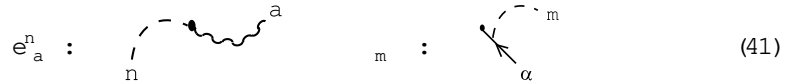
The use of graphs is popular in the history of mathematics and theoretical physics. Penrose [10], with the similar motivation described in the introduction, proposed a diagrammatical (graphical) notation in the tensorial and spinorial calculation. Feynman diagram is the most familiar graphical method to represent a scattering amplitude. The diagram tells us, without the explicit calculation, important features such as the coupling dependence, mass dependence and the divergence degree. Nakanishi [11] analysed the Feynman amplitude using the graph theory in mathematics. In this sense quite a large part of mathematical physics relies on the use of the graph.

As an application of the present approach, supergravity is interesting. Relating the full treatment to a separate work [12], we indicate a graphical advantage here. There appears such a quantity in the supergravity: $\mathcal{L} =$

$(^d) \cup (^c) \cup e_d^n e_c^m (_{nm}) ; (_{nm}) = \theta_{nm} +$ $n \neq m$: Graphically it is expressed as



where we introduce the graphical representation for the vierbein e_a^n and the Rarita-Schwinger field θ_{nm} as



The indices, which specifies the above graph (40), are given as follows: (LCN;RCN) = (3=2;1); (LUDN;RUDN) = (1=2; 1); (LWN;RWN) = (0;0); DIM = 5=2; DIF = 1; SIG = 2.

We have presented a graphical representation of the supersymmetric theory. It has some advantages over the conventional description. The applications are diverse. Especially the higher dimensional supergravities are the interesting physical models to apply the present approach. In the ordinary approach, it has a technical problem which hinders analysis. The theory is so "big" that it is rather hard in the conventional approach. The present graphical description is expected to resolve or reduce the technical but an important problem. We point out that the present representation is suitable for coding as a (algebraic) computer program. (See [13, 2] for the C-language program and graphical calculation for the product of Riemann tensors.)

Acknowledgment

The basic idea of this work was born during the author's stay at Albert Einstein Institute (fall of 1999). The author thanks the hospitality at the institute. He also thanks M. Abe, N. Ikeda, T. Kugo and N. Nakanishi for comments and criticism in the RIMS (Kyoto Univ.) workshop (2002.9.30-10.29). This work is completed in the present form in the author's stay during DAMTP (Univ. of Cambridge). He thanks the hospitality there. The author thanks G.W. Gibbons for comments and reference information. He also thanks S. Rankin for the help in computer work. Finally the author thanks the governor of the Shizuoka prefecture for the financial support.

References

[1] S. Ichinose, Class. Quantum Grav. 12 (1995) 1021, hep-th/9309035

[2] S. Ichinose and N. Ikeda, *Jour Math Phys.* 38 (1997) 6475, [hep-th/9702003](#)

[3] G.W. Gibbons and S. Ichinose, *Class. Quant. Grav.* 17 (2000) 2129, [hep-th/9911167](#)

[4] J. Wess and J. Bagger, *Supersymmetry and Supergravity*. Princeton University Press, Princeton, 1992

[5] S. Weinberg, *The Quantum Theory of Fields: Supersymmetry* (Volume III). Cambridge University Press, Cambridge, 2000

[6] P.G.O. Freund, *Introduction to Supersymmetry*. Cambridge University Press, Cambridge, 1986

[7] P. West, *Introduction to Supersymmetry and Supergravity*. World Scientific, Singapore, 1990

[8] E.A. Mirabelli and M.E. Peskin, *Phys. Rev. D* 58 (1998) 065002, [hep-th/9712214](#)

[9] A. Hebecker, *Nucl. Phys. B* 632 (2002) 101

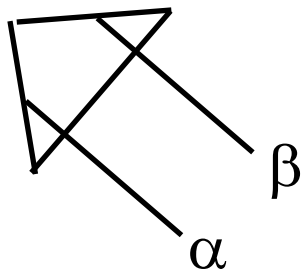
[10] R. Penrose, "Application of Negative Dimensional Tensors" in *Combinatorial Mathematics and its Applications*, 1971, ed. D.J.A. Welsh (Academic Press, London);
R. Penrose and W. Rindler, "Spinors and spacetime, Vol.1: Two-spinor calculus and relativistic fields", Cambridge University Press, Cambridge, 1984

[11] N. Nakanishi, "Graph Theory and Feynman Integral", Gordon and Breach, Science Publisher, New York-London-Paris, 1971

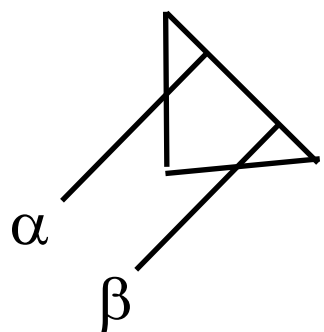
[12] S. Ichinose, in preparation.

[13] S. Ichinose, *Int. Jour. Mod. Phys. C* 9 (1998) 243, [hep-th/9609014](#)

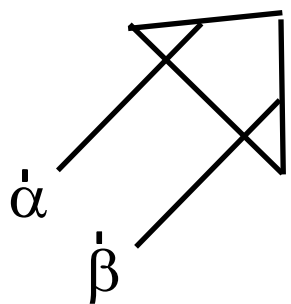
$$\varepsilon^{\alpha\beta}$$



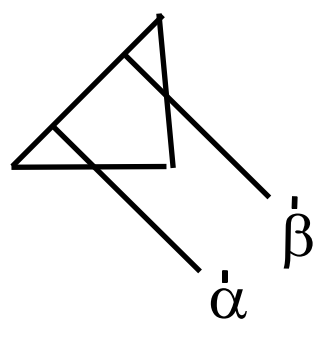
$$\varepsilon_{\alpha\beta}$$



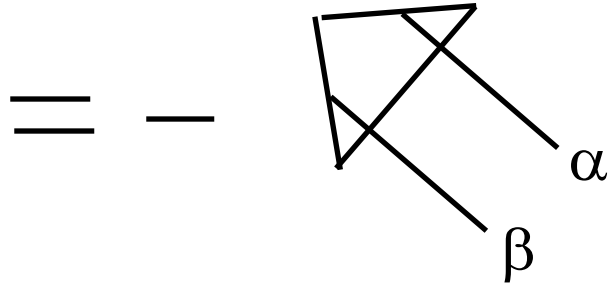
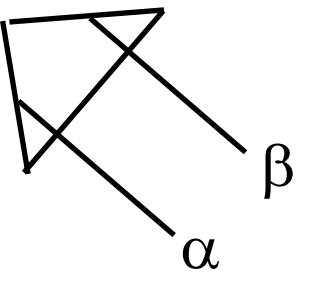
$$\varepsilon^{\dot{\alpha}\dot{\beta}}$$



$$\varepsilon_{\dot{\alpha}\dot{\beta}}$$

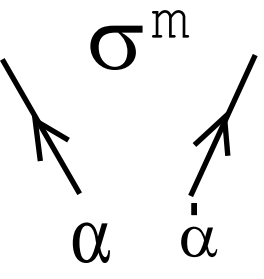


$$\varepsilon^{\alpha\beta} = - \varepsilon^{\beta\alpha}$$



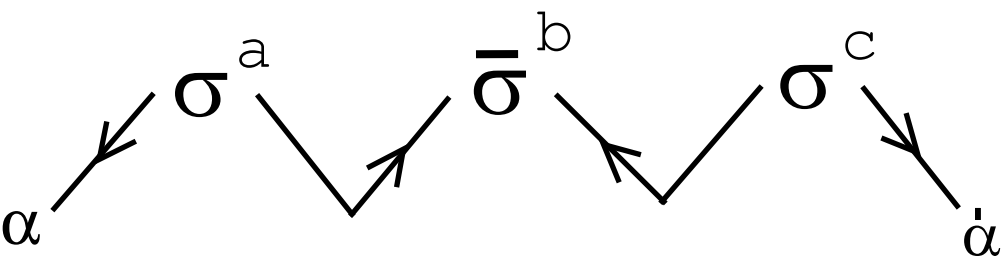
$\bar{\psi}$ $\bar{\xi}$

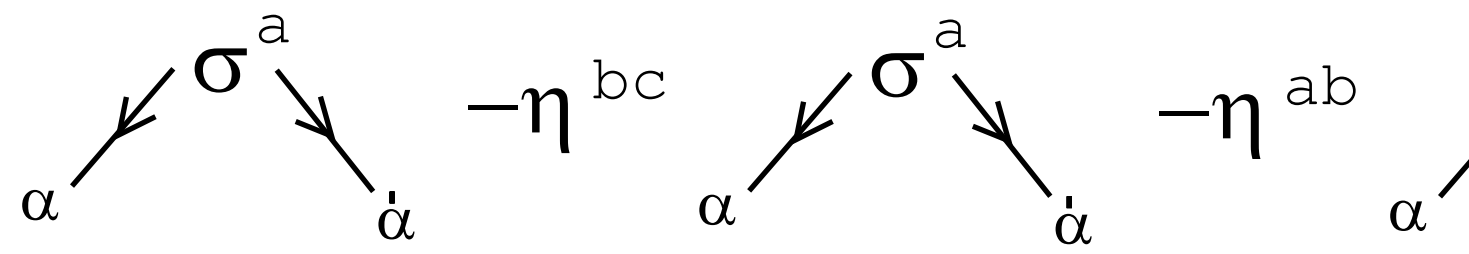
$$\dot{\alpha} \nearrow \bar{\sigma}^m \searrow \alpha$$



$\dot{\alpha}$ $\bar{\sigma}^m$ α

$$\alpha \nearrow \sigma^m \searrow \dot{\alpha}$$



$$\eta^{ac} \quad \sigma^a \quad -\eta^{bc} \quad \sigma^a \quad -\eta^{ab} \quad \alpha$$


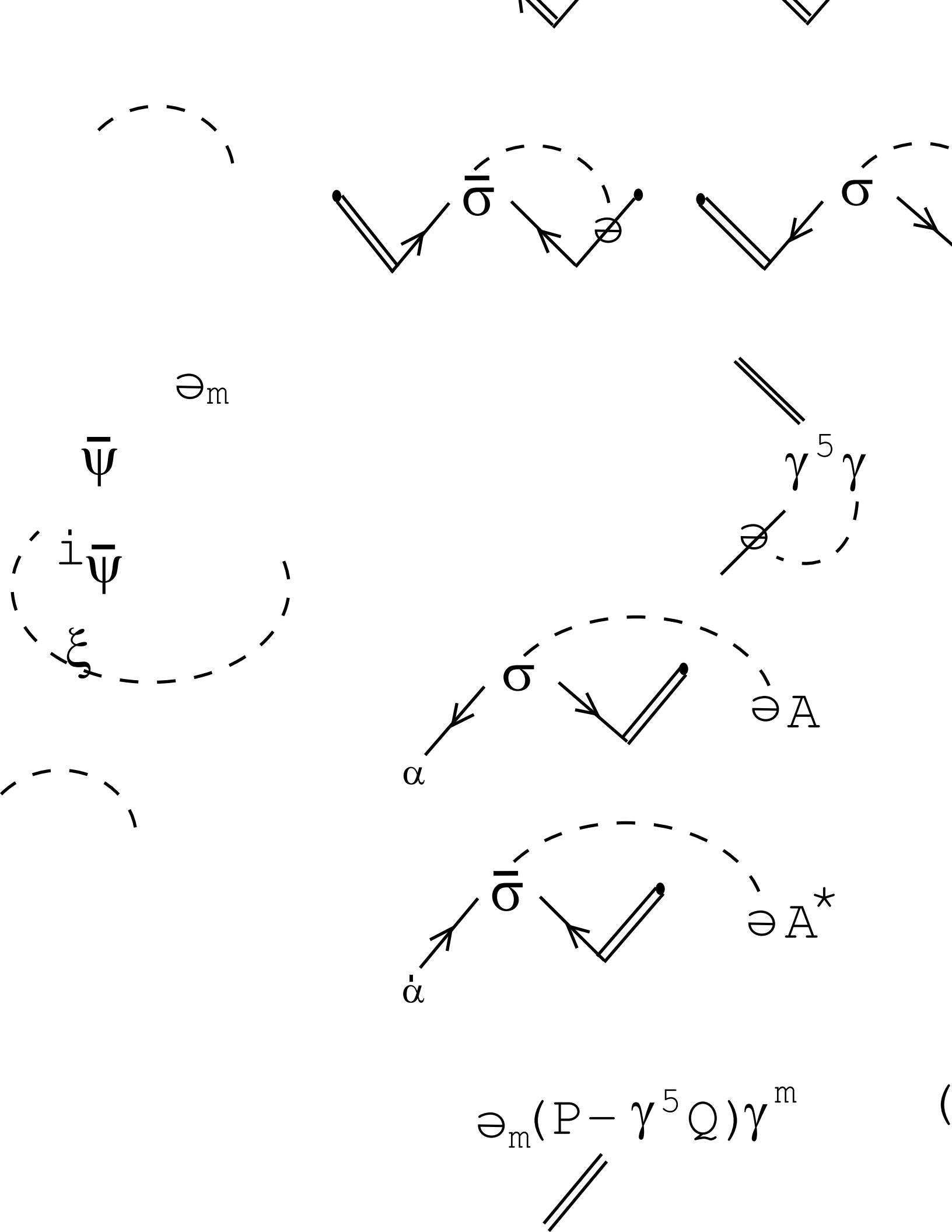
The diagram consists of two sets of curved arrows. The first set starts from the label α and points to the terms σ^a and $-\eta^{bc}$. The second set starts from the term σ^a and points to the terms $-\eta^{ab}$ and α .

$$\Psi^\alpha \equiv \epsilon^{\alpha\beta} \Psi_\beta$$

$$\Psi_\alpha \equiv \epsilon_{\alpha\beta} \Psi^\beta = - \Psi^\beta \epsilon_{\beta\alpha}$$

$$\bar{\Psi}^{\dot{\alpha}} \equiv \epsilon^{\dot{\alpha}\dot{\beta}} \bar{\Psi}_{\dot{\beta}} = - \bar{\Psi}_{\dot{\beta}} \epsilon^{\dot{\beta}\dot{\alpha}}$$

$$\bar{\Psi}_{\dot{\alpha}} \equiv \epsilon_{\dot{\alpha}\dot{\beta}} \bar{\Psi}^{\dot{\beta}}$$



$$\begin{array}{c} \text{Diagram: Two triangles with a diagonal line connecting them. The left triangle is labeled } \alpha \text{ and the right triangle is labeled } \beta. \\ = \\ \text{Diagram: Two triangles with a diagonal line connecting them. The left triangle is labeled } \alpha \text{ and the right triangle is labeled } \beta. \end{array} = \delta_{\beta}^{\alpha}$$

$$\begin{array}{c} \text{Diagram: Two triangles with a diagonal line connecting them. The left triangle is labeled } \alpha \text{ and the right triangle is labeled } \beta. \\ = - \\ \text{Diagram: Two triangles with a diagonal line connecting them. The left triangle is labeled } \alpha \text{ and the right triangle is labeled } \beta. \end{array} = 2$$

$$\begin{array}{c} \text{Diagram: Two triangles with a diagonal line connecting them. The left triangle is labeled } \dot{\alpha} \text{ and the right triangle is labeled } \dot{\beta}. \\ = \\ \text{Diagram: Two triangles with a diagonal line connecting them. The left triangle is labeled } \dot{\alpha} \text{ and the right triangle is labeled } \dot{\beta}. \end{array} = \delta_{\dot{\alpha}}^{\dot{\beta}}$$

$$\begin{array}{c} \text{Diagram: Two triangles with a diagonal line connecting them. The left triangle is labeled } \dot{\alpha} \text{ and the right triangle is labeled } \dot{\beta}. \\ = - \\ \text{Diagram: Two triangles with a diagonal line connecting them. The left triangle is labeled } \dot{\alpha} \text{ and the right triangle is labeled } \dot{\beta}. \end{array} = 2$$

